Finite-size effects on superlattice acoustic phonons

M. W. C. Dharma-wardana, P. X. Zhang,* and D. J. Lockwood
Institute for Microstructural Sciences, National Research Council, Ottawa, Ontario, Canada K1A 0R6
(Received 1 March 1993)

The high-resolution Raman spectrum of a $Si/Si_{1-x}Ge_x$ superlattice with $N=15$ periods has been studied. It is shown that the principal, secondary, and fine-structure features in the acoustic-phonon spectrum can all be consistently understood within a linear-chain model using first-principles force constants. The physical appearance of the features is very sensitive to N for $N<20$. It is also pointed out that simpler theories (e.g., Rytov model) would fail to predict the secondary structure and the fine structure, and the superlattice layer parameters fitted to the observed principal spectrum would be different from the true values. Thus it is important to use a detailed theory in using Raman spectra as a tool for the reliable characterization of microstructures.

I. INTRODUCTION

Since the beginning of semiconductor superlattice technology, Raman-scattering spectroscopy has proven to be an essential technique both for characterizing the superlattice structure and for investigating the physics involved.[1] A large part of this work has involved inelastic light scattering from acoustic phonons in superlattices. The effect of the artificially introduced periodicity d along the superlattice growth direction is to produce a Brillouin zone (minizone) much smaller in size (the maximum wave vector $q_{\max}=\pi/d$) than the original Brillouin zone of $q_{\max}=2\pi/a$, where a is the lattice constant. The acoustic phonons with a wave vector along the superlattice growth direction can be simply thought of as resulting from the folding back of the original lattice dispersion curve into the minizone. A very commonly used method for the calculation of phonon dispersion curves is to use the elastic continuum model of Rytov:[2,3]

$$\cos(qd)=\cos\left[\frac{\omega d_1}{v_1}\right]\cos\left[\frac{\omega d_2}{v_2}\right]-\frac{R^2+1}{2R}\sin\left[\frac{\omega d_1}{v_1}\right]\sin\left[\frac{\omega d_2}{v_2}\right]. \quad (1)$$

Here q and ω are the phonon wave vector and frequency, d_1,d_2 and v_1,v_2 are the thicknesses and sound velocities of the two-component layers of the superlattice, $R=\rho_2 v_2/\rho_1 v_1$, and ρ_1 and ρ_2 are the densities of the two layers. This model has been remarkably successful in predicting the acoustic properties of a large variety of semiconductor superlattices.[1,4]

The Rytov model is intrinsically a continuum model, and Eq. (1) is thus derived for the case where the number of superlattice periods $N\to\infty$. Experimentally, it has been shown that Eq. (1) is an excellent fit to the measured dispersion in cases where N is at least 20 and the experimental resolution is not too high (≥ 0.5 cm^{-1}).[4] It is also necessary that the layer thicknesses d_1 and d_2 are large enough if bulk velocities v_1 and v_2 or values derived from them are to be used. When the number of periods N becomes small, a detailed description of the spectrum requires a complete modeling of the microstructure inclusive of substrate, finite superlattice, and the cap, which is usually a few atomic layers of one of the two materials forming the superlattice. The need to do such modeling was emphasized in Ref. 5 where optical phonons in Ge_mSi_n superlattices were discussed. It was also shown in Ref. 6 that a complete finite-structure modeling was necessary to describe the acoustic-phonon spectra of 10-period Ge_2Si_2 and Ge_4Si_4 superlattices, which showed Fabry-Pérot type resonant-phonon phenomena due to substrate and capping layer effects on the phonon spectrum. Such resonance properties are entirely due to finite-size effects and their treatment is delicate. Similarly, acoustic-phonon spectra of finite-stage Fibonacci superlattices of $GaAs/Al_{1-x}Ga_xAs$ could only be interpreted[7] using a full calculation that did not invoke the $N\to\infty$ periodicity. Recently, high-resolution studies of thick-layer $Si/Si_{1-x}Ge_x$ superlattices have shown additional structure as well as fine structure in the acoustic-phonon Raman spectrum that cannot be explained by the Rytov model.[8,9] Also, the gaps that appear in the phonon disperson at $q=q_{\max}$ can only be fitted to a Rytov model by reducing the known values of v and ρ for Si by $\sim 1\%$ and increasing those for $Si_{1-x}Ge_x$ by $\sim 5\%$,[10,11] and even then the agreement with experiment is not up to expectations.

The fine structure that appears in the higher-resolution (<0.5 cm^{-1}) Raman spectra comprises splittings of the main folded acoustic-phonon peaks and numerous weaker peaks in between the main features.[8,9] These fine structures have previously been explained by assuming that the growth process had not produced the expected crystal and contained a variation in the superlattice period[8,9,11] and also that there are resonant modes of the entire superlattice structure.[9,11] Here, we analyze the high-resolution Raman spectra with a linear-chain lattice dynamical model[5,7] that explicitly includes the finite-size effects of the crystal. It is shown that the microscopic model accounts for all features of the experimental spectra in a systematic and coherent fashion. If the superlattice layers i and j have layer thickness fluctuations Δd_i

and Δd_j, the Raman spectrum is sensitive to the correlated fluctuation $\langle \Delta d_i \Delta d_j \rangle$. The general agreement between the observed spectra and the microscopic model results suggest that the molecular-beam epitaxy (MBE) growth has produced the target crystal with $\langle \Delta d_i \Delta d_j \rangle \simeq 0$, although the mean (random) layer fluctuation[11] $\langle |\Delta d_i| \rangle$ is of the order of 2%. The previous analysis[12] of the Raman spectrum was motivated by the disagreement with the Rytov model. We now believe that the shortcomings are in the Rytov model, which assumes an infinite-period superlattice, and not in the MBE-grown crystal, which is really a finite-period superlattice (FPSL). Thus the use of a proper detailed model can lead to conclusions that are diametrically opposite to what may be indicated by a simplified model. Similar size effects have been observed[13] in the electronic spectra of FPSL's.

II. HIGH-RESOLUTION RAMAN SPECTRA OF A 15-PERIOD $Si/Si_{1-x}Ge_x$ SUPERLATTICE

If the number of periods N in the FPSL is sufficiently large, but not large enough to be in the Rytov regime, finite-size effects on the Raman spectra of acoustic phonons would be a secondary effect modulating the strong scattering from the accumulation of modes which finally become the folded modes. To observe it, a high-resolution Raman spectrometer is necessary. In fact, we have used two double-grating spectrometers to obtain the acoustic-phonon spectra: a Spex 14018 and a SOPRA DMDP2000. The spectra obtained by the Spex 14018 were just like the usual folded acoustic-phonon spectra[4] and no special features were observed with a resolution of ~ 0.5 cm^{-1} while that obtained by the SOPRA DMDP2000 revealed considerable fine structure.[8,10]

As an example, we consider here a 15-period $Si/Si_{1-x}Ge_x$ superlattice with $d_{Si} = 20.5$ nm, $d_{Si_{1-x}Ge_x} = 4.9$ nm, and $x = 0.48$.[10] Figure 1 shows spectra obtained with the SOPRA DMDP2000 using 300 mW of laser excitation at 496.5 and 476.5 nm recorded in a Brewster angle pseudobackscattering geometry at room temperature. The sharp intense peaks in Fig. 1 correspond approximately to the pairs of folded phonons of Rytov theory[10,11] and their positions shift with varying laser frequency due to the change in the scattering wave vector of light. These peaks exhibit splittings, and other weaker but sharp features are observed between them.

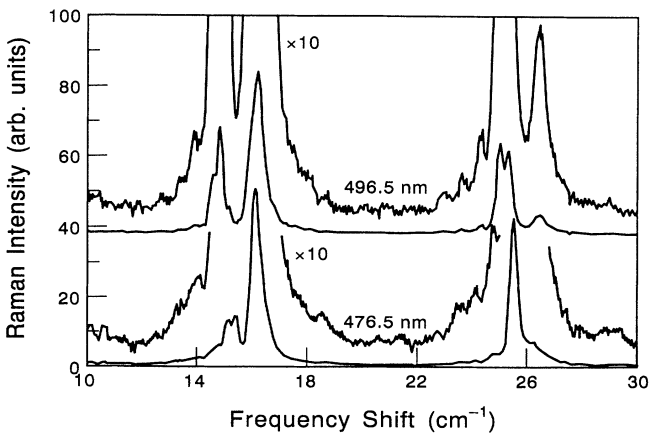

FIG. 1. Part of the Raman spectra of folded acoustic phonons in a 15-period $Si/Si_{0.52}Ge_{0.48}$ superlattice excited with 476.5- and 496.5-nm argon laser light recorded at a resolution of 0.18 and 0.15 cm^{-1}, respectively.

III. THEORY

A. Rytov model

As mentioned in Sec. I, the Rytov model is simple and widely used for discussing the basic physical properties of acoustic modes in superlattices. It was first developed by Rytov[2] from a study of sound wave propagation in layered structures. For simplicity, he took two component layers and arranged them in a periodic manner. One of the conditions of this model is that the wavelength of the sound wave should be much larger than the layer thickness. The elastic continuum approximation is then valid and the wave equation in each layer can be solved. By further applying periodic boundary conditions to the layered structure, Rytov obtained Eq. (1).

Following the development of artificial superlattices, it was found that the Rytov model could be used to describe the acoustic phonons in semiconductor superlattices.[3] The structure is regular and periodic, and in most cases the wavelengths of the acoustic phonons are larger than the thicknesses of the component layers.

Rytov theory predicts two important differences between acoustic phonons in superlattices and phonons in the bulk component materials. First, the Brillouin zone is folded. This can be seen clearly from a simplified form of Eq. (1):

$$\omega(q) = v \left| q \pm \frac{2\pi m}{d} \right| , \tag{2}$$

where v is the superlattice sound velocity given by

$$v = d \left[\frac{d_1^2}{v_1^2} + \frac{d_2^2}{v_2^2} + \left(R + \frac{1}{R} \right) \frac{d_1 d_2}{v_1 v_2} \right]^{-1/2} \tag{3}$$

and $m = 0, 1, 2, \ldots$ is the folding index. Second, phonon energy gaps are opened at the folded Brillouin-zone center and boundary (at $q = \pi/d$). Notice that the very possibility of using the concept of a wave vector q, and energy dispersion $\varepsilon(q)$, are associated with full periodicity, which is strictly valid only for the limit $N \to \infty$.

B. Linear-chain model

If the growth direction of the superlattice is along a favored symmetry direction like the $\langle 100 \rangle$ direction, then it can be shown that the lattice dynamical problem can be exactly and rigorously reduced to a linear-chain model of interacting parallel atomic layers. The analysis is well known and is given in standard texts.[14] A discussion appropriate to superlattices, but assuming superperiodicity, is given in, for example, Ref. 3. Such models

require the interlayer force constants and the masses (average mass in each layer) as input parameters.

In our previous studies[5,7] we used a linear-chain model of the total structure

$$\text{substrate}+(A_mB_n)_N+\text{cap}\ ,$$

where the substrate was modeled by 500–1000 atomic layers of A=Si or B=Ge, as the case may be, while the Si cap of 50 Å was modeled by 37 atomic layers of Si. The first atomic layer of the substrate was assumed to be fully anchored, while the surface layer (last layer of cap) was treated as free or anchored, depending on a parameter σ, which specified the degree of anchoring. In the present problem A is Si, while B is an alloy layer of $Si_{1-x}Ge_x$ where x is, e.g., 0.48. The layer thicknesses d_1 and d_2 defined by the growth conditions were 20.5 and 4.9 nm, and corresponded to 151 atomic layers of Si and 35 atomic layers of alloy along the growth direction ⟨100⟩. Thus each superunit cell corresponded to 186 layers. Here the alloy monolayer thickness was taken to be 0.1408 nm using the bulk values for Si and Ge, and interpolating linearly for the composition $x=0.48$. Theoretical force constants k_1 to k_4 for bulk silicon[15] and germanium[16] up to fourth-neighbor interactions were used in the linear-chain model, with linear interpolation to $x=0.48$ for the alloy. For interactions between A (=Si) and B (=alloy) the arithmetic mean of the force constants was used. These force constants as used by us are reported in Table I of Ref. 5. In our calculations we do not assume any translational invariance, etc., but simply diagonalize a matrix that is of dimensionality equal to $N_{\text{sub}}+N_{\text{sup}}+N_{\text{cap}}$, where N_{sub}, N_{sup}, and N_{cap} are the number of substrate, superlattice, and cap atomic layers, respectively. The matrix is a banded matrix, since only a limited number of interactions, viz., up to fourth-nearest neighbor, are taken into account. In order to keep the total size of the matrix relatively small we used $N_{\text{sub}}=2000$, while there was no cap in these structures.

IV. COMPARISON OF THEORY AND EXPERIMENT

A. Principal peaks

Figure 2 presents the full experimental spectra, together with the spectra calculated using the linear-chain model. The intensities $I(\omega)$ of the model spectrum were calculated using the photoelastic model. Thus $I(\omega)$ is given by the following expression, which contains a finite-range Fourier transform:

$$I(\omega)\sim\sum_n\left|\sum_i P(x_i)U_n'(x_i)\exp(iqx_i)\right|^2 \times\frac{n(\omega)+1}{\omega}\frac{\Gamma/2\pi}{(\omega-\omega_n)^2+(\Gamma/2)^2}\ . \tag{4}$$

Here $n(\omega)$ is a Bose factor at room temperature, while $P(x_i)$ and $U_n'(x_i)$ are the photoelastic constant and the derivative of the phonon amplitude in the ith layer at the position x_i for the mode with energy ω_n. The Lorentzian broadening factor Γ was taken to be 0.1 cm^{-1}. The photoelastic constant $P(x_i)$ was taken to be unity for Si layers, and 10 for alloy layers. $U_n(x)$ and ω_n were obtained from the eigenvector solutions of the linear-chain problem. The scattering wave vector of light, q, is given by $q\approx 4\pi\eta\lambda^{-1}[1-(4\eta)^{-2}]$. The refractive indices η used in the calculations were 4.777, 4.423, and 4.273 at the wavelengths 458, 488, and 515 nm, respectively. Experiments and calculations were also done at two other laser frequencies.

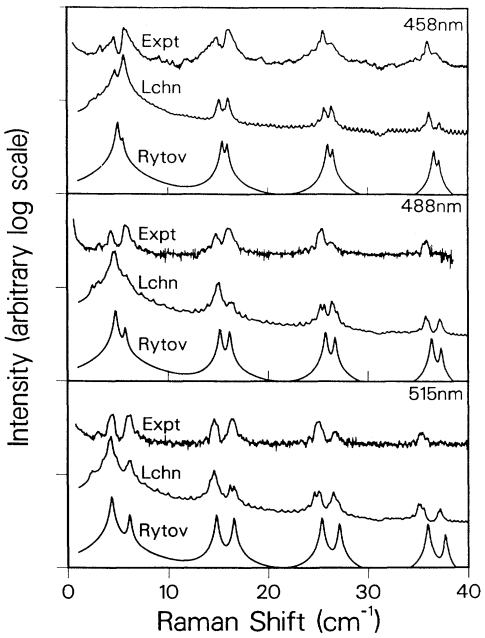

FIG. 2. Comparison of experimental and calculated Raman spectra in the $Si/Si_{0.52}Ge_{0.48}$ superlattice under different laser excitation wavelengths. In each box, the top trace is the experimental result (Expt), the middle trace is the linear-chain model result (Lchn), and the bottom trace is the Rytov model result (Rytov).

The curve labeled Rytov in Fig. 2 was calculated using the photoelastic theory, analogous to that used in the theory of the linear chain, using $P_{\text{Si}}=1$ and $P_{\text{alloy}}=10$, employing the formulas of Ref. 3. It should be pointed out that this type of intensity theory is known to be inadequate and that the "superlattice" equations for the Maxwell equations also have to be solved in consort with the lattice dynamics equations to recover reliable intensity results. Thus the doublet intensities of the curves marked Lchn and Rytov in Fig. 2 are essentially equal, while this is not at all the case in the experimental data. However, the linear-chain calculation clearly reproduces the general features of the spectrum and the correct peak positions, without adjustment of the input parameters.

In solving the linear-chain problem, the behavior of the first atomic layer (first layer of the substrate) forming the chain, and the last atomic layer (i.e., the surface layer) specify the boundary conditions. In this calculation we assumed that the first layer (substrate) was fully anchored ($\sigma=1$), while the surface layer vibration was damped ($\sigma=0.1$). Unlike in optical mode calculations, the (long-wavelength) acoustic-phonon spectrum is not sensitive to the boundary conditions. Thus if the surface layer was allowed to vibrate freely ($\sigma=0$), or fully anchored ($\sigma=1$), no new features are explicitly seen in the part of

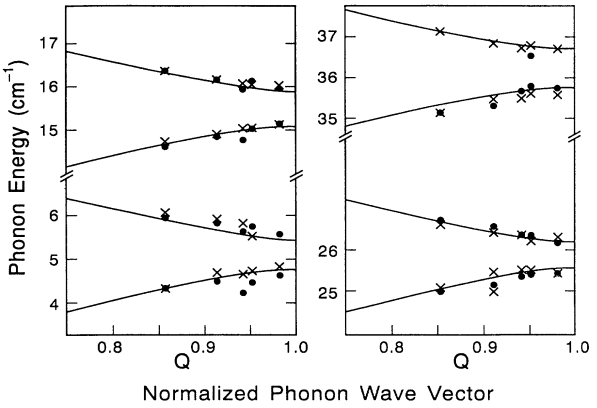

FIG. 3. Comparison of experiment and theory for the excitation wavelength dependence of the positions of major peaks in the folded acoustic-phonon Raman spectrum of the $Si/Si_{0.52}Ge_{0.48}$ superlattice: full circles, experiment; crosses, linear-chain model; solid lines, Rytov model. The normalized phonon-wave vector $Q=q/q_{max}$.

the spectrum under study, although some of the intensities of the fine structure around 30 cm^{-1} are found to change. Although the theory of Raman intensities is not well formulated, these features most likely arise from localized modes induced by the surface (see Sec. V). Since any surface modes tend to have short wavelengths (exponential decay away from the surfaces), it is expected that they would not show up in the long-wavelength regime studied here. All the calculations reported here assume $\sigma=1$ for the first (substrate) atom, and $\sigma=0.1$ for the surface atom.

B. Folded phonon representation

Figure 3 depicts part of the dispersion curves for the $Si/Si_{0.52}Ge_{0.48}$ superlattice calculated in the Rytov model using the best-fit superlattice parameters quoted in Ref. 11 (i.e., $\rho_{Si}=2.30$ g/cm^3, $\rho_{Si_{0.52}Ge_{0.48}}=4.06$ g/cm^3, $v_{Si}=8.35\times10^5$ cm/s, and $v_{Si_{0.48}Ge_{0.52}}=6.40\times10^5$ cm/s). The dispersion curves generally are a good fit to the experimental points, apart from the lowest ($m=1$) doublet. The results from the linear-chain model do not provide a wave vector, but only a mode index. However, for comparison purposes, the energies can be plotted at the same wave vector as the corresponding experimental results in a pseudo-wave-vector representation. This is done in Fig. 3 and it can be seen that the linear-chain model gives an equally good, if not slightly better, representation of the major experimental peaks. Note that in the Rytov model various parameters were adjusted to optimize the fit to experiment, while the linear-chain model has no adjustable parameters and uses the first-principles force constants scaled as discussed in Ref. 5.

V. DEPENDENCE OF THE SPECTRUM ON FINITE-SIZE EFFECTS

From the foregoing discussion it should be clear that the spectrum of the structure substrate$+(A_mB_n)_N$ would

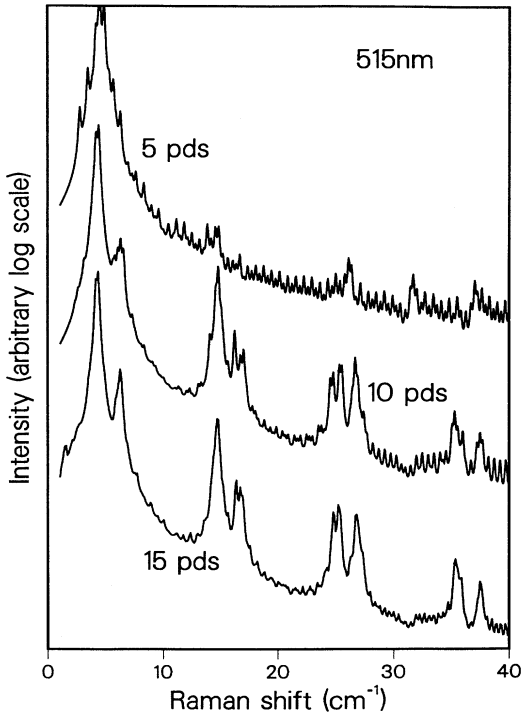

FIG. 4. Raman spectra of $N=5$-, 10-, and 15-period $Si/Si_{0.52}Ge_{0.48}$ superlattices calculated with the linear-chain model.

be a function of N that would finally evolve towards the fully periodic result as $N\rightarrow\infty$. The final folded modes are produced by the accumulation of a high density of states at certain energies of the mode spectrum. Thus Fig. 4 shows the calculated spectra, using the linear-chain model, for $N=5$, 10, and 15 periods, at the laser wavelength of 514.5 nm. The last case, $N=15$, corresponds to the present experimental sample. The case $N=5$ corresponds to such low intensities that the accumulation of modes close to the Rytov peak positions would not be observable above the fine structure, which defines an almost uniform distribution of modes. As N increases the fine structure persists, while the density of states near the Rytov peaks increase, increasing the intensity at those frequencies. It is also seen that the structural features associated with localized surface modes in the 30-cm^1 region change as N goes from 5 to 15, due to the decreasing effects of the surface.

VI. DETAILS OF FINE STRUCTURE

It is clear from Fig. 4 that the fine structure is a result of the finite-Fourier-transform effect contained in Eq. (4). Just as deviations from periodicity in ordinary x-ray spectra could lead to additional structure, the scattering of light from the different layers of the finite-N structure leads to a multiplicity of peaks, with the strongest signals coming from those frequencies corresponding to accumulations of a high density of modes. It should be emphasized that the *calculated* intensities given in these figures have only a qualitative significance since it is known that the simple photoelastic theory used in Eq. (4)

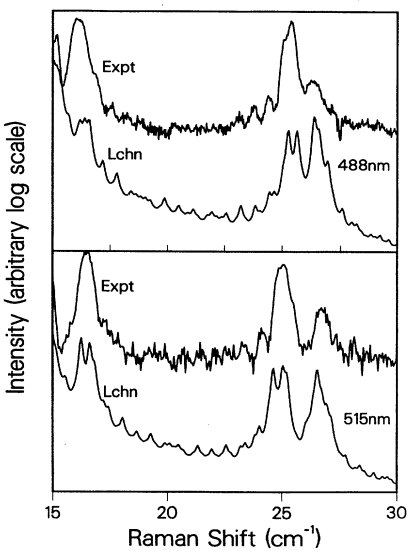

FIG. 5. Comparison of calculated (Lchn) and experimental (Expt) weak fine structure observed in the Raman spectrum of the $Si/Si_{0.52}Ge_{0.48}$ superlattice for different laser excitation wavelengths.

is inadequate, and also because we have scaled the very intense Brillouin peak and the relative intensities of the other peaks in order to present the information in a convenient graphical form.

In Fig. 5 we display the experimental fine structure and the calculated fine structure for two laser wavelengths for the range 15–30 cm^{-1}. The theoretical spectrum carries a broadening parameter of 0.1 cm^{-1} as already mentioned. It is clear that the qualitative agreement is strikingly good. At the quantitative level, the 488-nm spectrum is very satisfactory; the 515-nm spectrum is visually less satisfactory, since the apparant double peak structure shown in the *principle peaks* of the Lchn curve is not seen in the experiment. By returning to Fig. 2 it is easy to conclude that the broadening parameter of 0.1 cm^{-1} applied to the calculated structure may not be adequate for this case. If we ignore the fine structure on the principal peak, the interval between fine-structure peaks of the calculated spectrum and their positions seem to be in general agreement with the experiment. A more detailed assignment is not justifiable since the intensities are calculated with a limited theory and this affects the quality of the assignment. As already stated, a correct evaluation of the intensities requires the layer-by-layer solution of the Maxwell equations along the finite-sized superlattice. Such a solution for the Rytov case is quite tractable and has been given by He, Djafari-Rouhani, and Sapriel (see Ref. 1).

VII. CONCLUSIONS

The analysis of the high-solution experimental Raman spectrum of a finite-size superlattice has served to demonstrate the importance of detailed modeling when the spectrum shows deviations and fine structure not predicted by simpler theories. The linear-chain model used here has successfully predicted the principal- and secondary-peak positions, as well as the general features of the fine structure, without having to adjust the fitting parameters. In addition, considerable variation was found in the physical appearance of the calculated Raman spectrum depending on the number of superlattice periods. We conclude that this is of significance not only for elucidating the physics, but also for detailed characterization of microstructures by Raman methods.

ACKNOWLEDGMENTS

We thank J.-M. Baribeau for providing samples and H. J. Labbé for technical assistance in the experimental investigations reported earlier.[9–11] We thank G. C. Aers for many discussions, and for various aspects of the linear-chain code used here.

*On leave from the Institute of Physics, Chinese Academy of Sciences, Beijing, People's Republic of China.

[1]D. J. Lockwood and J. F. Young, *Light Scattering in Semiconductor Structures and Superlattices* (Plenum, New York, 1992).

[2]S. M. Rytov, Akoust. Zh. **2**, 71 (1956) [Sov. Phys. Acoust. **2**, 68 (1956)].

[3]C. Colvard, T. A. Gant, M. V. Klein, R. Merlin, R. Fisher, H. Morkoç, and A. C. Gossard, Phys. Rev. B **31**, 2080 (1985).

[4]J. Sapriel and B. Djafari-Rouhani, Surf. Sci. Rep. **10**, 189 (1989).

[5]M. W. C. Dharma-wardana, G. C. Aers, D. J. Lockwood, and J.-M. Baribeau, Phys. Rev. B **41**, 5319 (1990).

[6]D. J. Lockwood, M. W. C. Dharma-wardana, G. C. Aers, and J.-M. Baribeau, Appl. Phys. Lett. **52**, 2040 (1988).

[7]G. C. Aers, M. W. C. Dharma-wardana, G. P. Schwartz, and J. Bevk, Phys. Rev. B **39**, 1092 (1989).

[8]D. J. Lockwood, Surf. Sci. **267**, 438 (1992).

[9]P. X. Zhang, D. J. Lockwood, and J.-M. Baribeau, Appl. Phys. Lett. **62**, 267 (1993).

[10]P. X. Zhang, D. J. Lockwood, H. J. Labbé, and J.-M. Baribeau, Phys. Rev. B **46**, 9881 (1992).

[11]P. X. Zhang, D. J. Lockwood, and J.-M. Baribeau, Can. J. Phys. **70**, 843 (1992).

[12]Equation (3) given in Ref. 9 applies if the period d of a perfect superlattice is changed to $d+\Delta d$ of another perfect superlattice, and hence does not describe the effect of layer fluctuations, as was implied there. Similarly, the first approximation to the "resonant modes" of the whole superlattice are just the Rytov modes and we now believe that Eqs. (4) and (5) of Ref. 9 are not applicable.

[13]R. J. Aggarwal *et al.*, Appl. Phys. Lett. **57**, 707 (1990).

[14]C. Kittel, *Introduction to Solid State Physics* (Wiley, New York, 1971), Chap. 5.

[15]A. Fleszar and R. Resta, Phys. Rev. B **34**, 7140 (1986).

[16]K. Kunc, in *Electronic Structure, Dynamics and Quantum Structural Properties of Condensed Matter,* edited by J. Devreese and P. Van Camp (Plenum, New York, 1984), Table 5.1.